



## EXPERIMENTAL RESEARCH ON PHASE CHANGE REGENERATOR CONSISTING OF FLAT TUBE HEAT EXCHANGER AND SHAPE-STABILIZED PHASE CHANGE MATERIAL FOR SPACE APPLICATIONS

Jiahua Xu<sup>1</sup>, Zhenhui He<sup>2</sup>, Guangzhou Dang<sup>3</sup>

<sup>1</sup>School of Engineering, Sun Yat-Sen University, No. 135, Xingang Xi Road, Guangzhou, 510275, P. R. China

<sup>3</sup>Aerospace Institute of Advanced Materials & Processing Technology, Beijing 100074, P. R. China

<sup>1</sup>xujh36@mail2.sysu.edu.cn

<sup>3</sup>dgz9627@163.com

<sup>2</sup>School of Physics and Astronomy, Sun Yat-Sen University, Zhuhai 519082, P. R. China

<sup>2</sup>stshzh@mail.sysu.edu.cn

<https://doi.org/10.33329/ijer.71.1>



### ABSTRACT

For the applications in the thermal environments with wide temperature range, such as deep space explorations, phase change materials (PCM) provide an ideal solution to achieve a comfort environments. PCM can also provide solution for applications of instantly much higher cooling power with a limit electric power supply. In both cases, solid state or stabilized shape is helpful for PCM to achieve high thermal conductivity and avoid fluid management in microgravity. It is important to understand the heat transfer between the shape-stabilized PCM and the heat exchanger of such phase change regenerator (PCR), for the design and optimization of the PCR. In this paper, experimental investigation was performed to a home-made PCR to understand its performance of cold storage and cold release to liquid flow in the heat exchanger.

**Keyword**—space applications, shape-stabilizedPCM , flat-tube HX, PCR, liquid flow.

### 1. INTRODUCTION

In space applications, spacecrafts or payloads have strict constraints on resources such as mass budget and power budget in complex thermal environments. Phase change cold storage technology provides valuable options [1]. In the spacecraft on the Nimbus orbit, Fixler [2] compared the phase change material device with other cooling methods to prove that phase change material devices have a great advantage in reducing weight. In the Apollo-15 mission, the lunar rover used three sets of phase change material for the thermal controls [3]. In 2016 on the International Space Station, NASA demonstrated and tested a phase

change heat exchanger with PCM of N-pentadecane which achieved cold storage density of 200 kJ/kg. Although with large latent heat, low thermal conductivity makes pure paraffin hard to store and release power with high thermal flux. In addition, after melt, liquid paraffin makes it difficult to store and manage in the microgravity. To improve the thermal conductivity of paraffin, it was extensively studied and applied by adding Carbon-based materials [4]. For example, Tian et al. [5] proved the significantly synergistic enhancement of thermal conductivity of Carbon-based materials by using expanded graphite (EG) and carbon fiber (CF) with different mass ratio. At the same time, shape-stabilized PCM was made in this way, keeping itself

solid even in the process of cold energy release.

Compact in structure, light in weight, and high in heat transfer efficiency [6], fin-flat tube heat exchanger is a popular kind of heat exchange equipment widely used in automotive air conditioning. It consists of flat tubes, collectors and wavy fins. Flat tubes have high heat exchange coefficients with the condensing working fluid. Therefore researches were concentrated on optimizing air-side thermal hydraulic performance to improve the overall efficiency of heat exchange [7, 8]. The condensation heat transfer was also studied by simulation for R134a with low mass flow inside a horizontal single square minichannel [9]. Few studies was published to apply flat tube heat exchanger to PCR, but the PCM was filled inside the flat tube[10]. In this research, we develop a PCR based on aluminum microchannel flat tube heat exchanger, in which the wavy fin heat sink was replaced by the shape-stabilized PCM. The cold storage quantity of the PCR were characterized. The cold release efficiency and the cold release heat transfer capacity of the PCR were investigated for liquid flow.

## II. EXPERIMENTAL

### 2.1 Structure of the phase change regenerator

The developed PCR consisted of four blocks of PCM, a PCM heat exchanger (PCM HX), and four chips of Thermal Electric Cooler [TEC 12706, Thermoamic Electronics (Jiangxi) Corp., Ltd] with water cooled heat sink on the hot sides, as shown in the Fig. 1.

The PCM block was made of alkane-type N-tridecane absorbed in expanded graphite (EG) that was shape-formed at a high temperature. One of PCM blocks is thicker than the other three. Thermal grease were applied to the interfaces between the base plate of the PCM heat exchanger and the TEC chips, and those between the PCM blocks and the PCM heat exchanger to reduce the contact thermal resistances. To measure the temperatures, six pairs of thermocouple were installed on the PCM blocks near the inlet and the outlet of the PCM HX. Three were mounted on the thicker PCM at the position 1, 2, and 3, while the other three at the position 4, 5, and 6, as shown in the Fig. 2. They represent the

positions that the closest to, and the farthest away, from the PCM HX during cold storage or cold release processes.

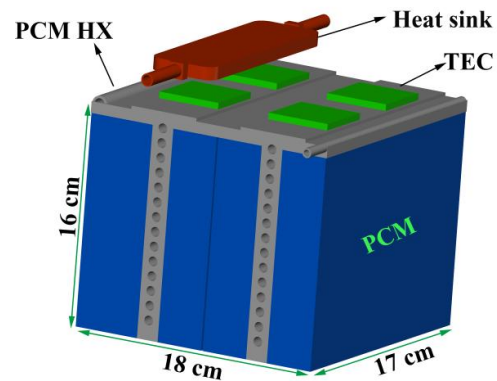


Fig. 1 The structure of the PCR

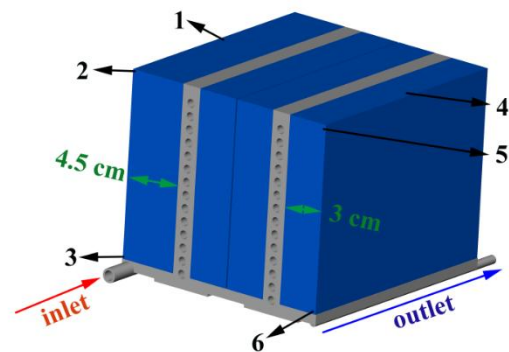


Fig. 2 The mounting positions of the thermocouples

### 2.2 Loop principle

To investigate the PCR, an experimental bench was built. As shown in the Fig. 3, it consists mainly a pump, a flowmeter, an electric preheater, and an accumulator. The pump (MICROPUMP,GA-T23.PVS.M) is used to drive the refrigerant fluid to cycle along the loop. The flowmeter (Bronkhorstminicori,M15-AAD-33-0-S, precision of 0.2%FS) is used to measure the mass flow rate. The preheater (up to 300W, with precision of 1.4%) is used to put thermal power into the fluid to control the fluid's temperature in liquid state. The accumulator, a vessel made of 316 stainless steel, is used to control the pressure of the loop by controlling the accumulator temperature, and to compensate the change of vapor volume of the working fluid in different cases. The working fluid was R134a (DuPont SUVA 134a). The mass flow rate was adjusted by controlling the rotation speed of the

pump, or by adjusting the valve<sub>R</sub> between the flowmeter and the preheater. Temperature was acquired by FLUKE 2680A, with sampling rate of 1Hz. In addition to the mounted thermocouples on the PCM, some other thermocouples were mounted along the loop. Sheathed thermocouples were inserted in the loop to directly measure the fluid temperatures at the inlet of the preheater, the inlet and the outlet of the PCR.

Performances of the PCR were investigated for both processes of "cold storage" and "cold release". The process of "cold storage" refers to the heat extraction from PCM with the TEC, so as to achieve the cold storage. At first, the temperature of the cycling water (from the thermostatic bath, HX-15D, Beijing Fortunejoy Science Technology co.,) was set at 25 °C. Then the TEC was turned on, with the input current of 3A. The main parameters of the TEC are listed in Table 1. The cooling capacity on the cold side of the TEC was calculated by the following formula[11]:

$$Q_{TEC} = \alpha I(T_c + 273.15) - K(T_h - T_c) - \frac{1}{2} I^2 R \quad (1)$$

Where  $\alpha$  is the average Seebeck number of TEC; K is the total heat conductivity in the direction of the heat flow; R is the average resistance of the TEC;  $T_h$  and  $T_c$  is the temperature of the TEC hot side and cold side, respectively.

Table 1 Main parameter of TEC[12]

No.	Parameter	Value	Description
1	Size ( mm <sup>3</sup> )	40×40×3.8	
2	$\alpha$ ( V/ °C )	0.054	The average Seebeck number of TEC
3	$K$ ( W/ °C )	0.0549-0.0014( $T_h - 27$ )	Total heat conductivity in the direction of heat flow, relative to hot side temperature of TEC
4	$R$ ( $\Omega$ )	2.01+0.006( $T_h - 27$ )	The average resistance of TEC

$$T_c = \frac{1}{2} (T_6 + T_3) \quad (2)$$

Actually  $T_c$  was close to the temperature at the

PCM position 3 and 6 in Fig.2 near the base plate. Its value should be approximately equal to the mean temperature at the positions.

In the process of cold storage, the valve and the pump were closed. The TECs took away the heat from the PCM to the cooling water through the TEC heat sink, then to the thermostatic water bath A.

"Cold release" refers to the process that hot fluid is cooled by the cold PCM after it flows through the PCR, even without TEC cooling. In the cold release process, the PCM near the inlet of the PCR melt fastest, and the data we discussed are all before its complete melting. At this time, all PCM inside PCR participate in the heat transfer in the latent heat. And combined with the actual application, the outlet temperature reaching 5°C was defined to be the end of the cold release.

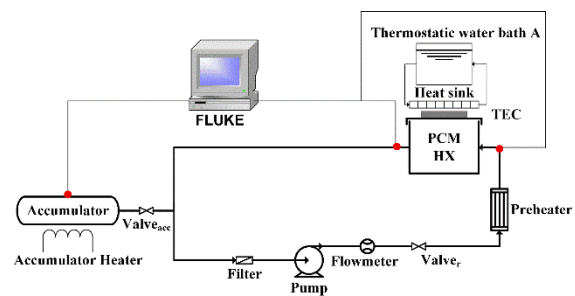


Fig. 3 Schematic drawing of the experimental bench

### III. DATA ANALYSIS METHODOLOGY

#### 3.1 Cold storage quantity

The cold release power from the PCM to the fluid through the PCR can be calculated from the temperature difference between the inlet and the outlet of the heat exchanger, and the mass flow rate of the fluid. The cold storage quantity of the PCR  $Q_{cs}$  (kJ/kg) is thus obtained by the integration of the cold release power over the cold release period:

$$Q_{cs} = \int_{t_i}^{t_e} \dot{m} c_p \Delta T_1 dt \quad (3)$$

Where  $t_i$  is the time to turn on the pump and the valve,  $t_e$  is the time when the lowest temperature of PCM rises to -4.0 °C,  $\dot{m}$  and  $c_p$  is

respectively the mass flow rate and the specific heat of the fluid,  $\Delta T_1$  is the temperature difference between the inlet and the outlet of the heat exchanger. Here,  $Q_{cs}$  includes the latent heat of the PCM and the sensible heat of the PCR.

### 3.2 Cold release capacity

The cold release capacity of the liquid flow is defined as the thermal power of the heat exchange under certain temperature difference between the PCM cold end and the fluid through the PCR. In the "cold release" process, the cold release power ( $P_{cr}$ ) to the liquid can be calculated if we know the mass flow rate ( $\dot{m}$ ) and the specific heat ( $c_p$ ) of the liquid through the PCR, and the temperature difference of the liquid between the inlet of the preheater and the outlet of the PCR. Then the cold release capacity of the regenerator can be obtained as:

$$\frac{dP_{cr}}{dT} = \frac{\dot{W} - \dot{m}c_p(T_{out} - T_{pre\_in})}{\bar{T}_H - \bar{T}_L} \quad (4)$$

Where  $\dot{W}$  is the heating power of the preheater,  $T_{pre\_in}$  is the temperature at the inlet of the preheater,  $\bar{T}_H = \frac{1}{2}(T_{out} + T_{in})$  is the average temperature of the fluid through the PCR, and  $\bar{T}_L = \frac{1}{4}(T_1 + T_2 + T_4 + T_5)$  is the average temperature over the PCM cold ends,  $T_{out}$  and  $T_{in}$  is respectively the fluid temperature at the outlet and the inlet of the PCR.

## IV. DISCUSSION OF RESULTS

### 4.1 PCM performance

During the process of "cold storage" and "cold release", the PCM undergoes endothermic and exothermic processes, respectively. As can be seen in Fig. 4, after the TEC is turned on, the temperature of the PCM begins to drop rapidly. The phase transition temperature of the PCM is approximately -5 °C. However, the temperature is not constant, but a slight decline in the process of cold storage, when the temperature is between -4°C and -5°C. Temperatures at position 1, 2, and 3 drop slower than those of the other three. This is reasonable because position 1, 2, and 3 are on the thicker PCM block. Therefore, when the highest temperature of the PCM block drops below -5 °C, the cold storage process was regarded as finished. For the applied

current to TEC of 3A, and the temperature of the heat sink cooling water of 25 °C, the time for cold storage was approximately 3.6 h. The time can be shortened to 2.2 h when the temperature of the cooling water was 10 °C. The cold release is with liquid R134a at the mass flow rate of 2.0g/s.

Based on data of the cold release process and equation (3), the cold storage quantity was calculated to be about 346 kJ, and the measurement error from the instruments was less than 2%. The mass of the PCM, the PCM HX, and the heat sink with TEC is 2.6kg, 1.7kg, and 0.4kg, respectively. The measured cold storage density of the PCM was about 130 kJ/kg, equivalent to a density of 80.5 kJ/kg, or 73.6 kJ/kg for the whole PCR if the TECs cooling device and heat sink were included, respectively.

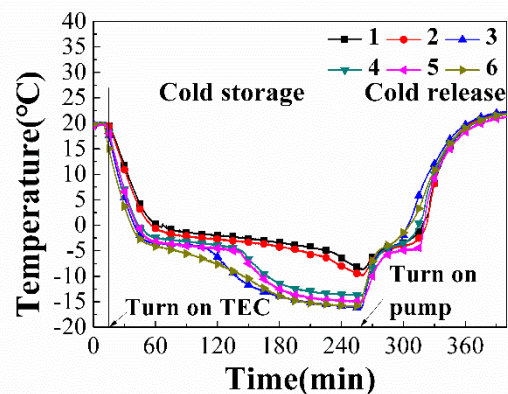


Fig. 4 Temperature changes at the defined positions of the PCM blocks in Fig.2

### 4.2 Cold release capacity

The effect of fluid mass flow rate on cold release capacity was investigated. The loop pressure was stabilized at 720 kPa when the accumulator temperature was adjusted to 28 °C. The inlet temperature of the PCM HX was set as 25 °C to make sure that the inlet flow was liquid phase. As shown in Fig.5, there is a positive correlation between the cold release capacity and the mass flow of the fluid. When the mass flow reaches 4.0 g/s, there was a peak of cold release capacity at the beginning, before it falls down and becomes flat. The flat cold release processes last for about one hour, indicating that the PCR could provide stable low temperature and low flow rate liquid for one hour, depending on the mass flow rate of the fluid. Since



there was fluid already cooled inside the PCM HX, it took time to establish a steady cold release process that equation (4) is suitable to. The lower the mass flow rate was, the longer the process got steady.

The cold release capacity depends on the cold energy available in the PCM, and the thermal resistance between the PCM melting interface and the PCM HX. For liquid flow, the cold energy in the PCM is adequate, thus the cold release capacity mainly depends on the thermal resistance. At this moment, the "melting interface" inside the PCM is close to the surface of the PCM HX, giving a low thermal resistance between the R134a and the unmelted PCM. Therefore, the thermal resistance is mainly from liquid side, especially at low mass flow rate. As the mass flow increased from 0.6 g/s to 6.0 g/s, the Reynolds number in the flat tube also increased from 33 to 330. The frictional resistance, and the heat exchanging coefficient increases with the mass flow rate for rough tubes [13-15], resulting in the increase of the cold release capacity. As the PCM melts, the melting interface withdraws from the surface of the PCM HX, and the thermal resistance increases correspondingly. The thermal resistance of the PCM becomes higher than that of the liquid flow, and becomes the main factor that dominates the heat exchange coefficient. At this moment, the cold release capacity decreases to that matches the PCM thermal resistance. This leads to a peak in the cold release capacity curve.

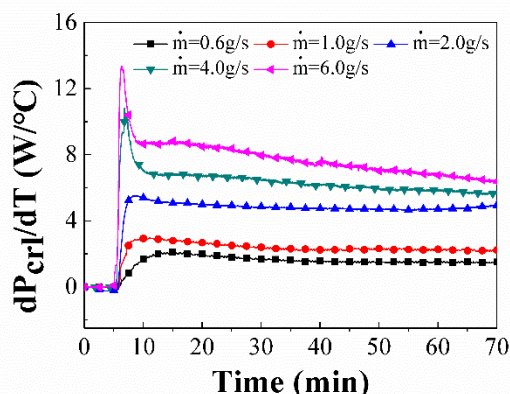


Fig. 5 Cold release capacity of liquid flow at different mass flow rate of R134a

## V. CONCLUSIONS

In this study, we investigated the thermal performance of a PCR that consists of an aluminum

flat tube as heat exchanger and the shape-stabilized PCM. The PCM's phase transition temperature was approximately -5°C, and the measured cold storage density was about 130 kJ/kg. The cold storage quantity of the PCR was about 346 kJ, equivalent to a density of 80.5 kJ/kg; or 73.6 kJ/kg if the TECs cooling device and heat sink were included. The cold release capacity was about 6.0 W/°C for liquid with mass flow rate of 4.0 g/s.

## ACKNOWLEDGEMENT

This work was supported by the Project of ChinaManned Space Station Engineering.

## REFERENCES

- [1]. Swanson T D, Birur G C. NASA thermal control technologies for robotic spacecraft[J]. Applied Thermal Engineering, 2003, 23(9): 1055-1065.
- [2]. Fixler S Z. Satellite thermal control using phase-change materials[J]. Journal of Spacecraft & Rockets, 2015, 3(9): 1362-1368.
- [3]. Biswas D R. Thermal energy storage using sodium sulfatedecahydrate and water ☆[J]. Solar Energy, 1975, 19(1): 99-100.
- [4]. Lin Y, Jia Y, Alva G, et al. Review on thermal conductivity enhancement, thermal properties and applications of phase change materials in thermal energy storage[J]. Renewable and Sustainable Energy Reviews, 2018, 82: 2730-2742.
- [5]. Tian B, Yang W, Luo L, et al. Synergistic enhancement of thermal conductivity for expanded graphite and carbon fiber in paraffin/EVA form-stable phase change materials[J]. Solar Energy, 2016, 127: 48-55.
- [6]. Delač B, Trp A, Lenić K. Numerical investigation of heat transfer enhancement in a fin and tube heat exchanger using vortex generators[J]. International Journal of Heat and Mass Transfer, 2014, 78: 662-669.
- [7]. Liu J, Jiang Y, Wang B, et al. Assessment and optimization assistance of entropy

- generation to air-side comprehensive performance of fin-and-flat tube heat exchanger[J]. International Journal of Thermal Sciences, 2019, 138: 61-74.
- [8]. Dezan D J, Salviano L O, Yanagihara J I. Interaction effects between parameters in a flat-tube louvered fin compact heat exchanger with delta-winglets vortex generators[J]. Applied Thermal Engineering, 2015, 91: 1092-1105.
- [9]. Li P P, Chen Z Q, Shi J. Numerical Study on the Effects of Gravity and Surface Tension on Condensation Process in Square Minichannel[J]. Microgravity Science and Technology, 2018, 30(1-2): 19-24.
- [10]. Chen C Q, Diao Y H, Zhao Y H, et al. Experimental and numerical investigations of a lauric acid-multichannel flat tube latent thermal storage unit[J]. International Journal of Energy Research, 2018, 42(13): 4070-4084.
- [11]. Yang M W, Wen-Hai X U, Tang W Y. Modeling and analysis of thermoelectric cooler by equivalent circuit method[J]. Infrared & Laser Engineering, 2007, 36(2): 281-285.
- [12]. Wang Z, Zhang X, Wen S, et al. Space Application of Pumped Two-Phase Temperature Control System Combined with TEC(in Chinese)[J]. Journal of Astronautics, 2018, 39(10): 1176-1184.
- [13]. Ma C, Yuan H, Sun L, et al. The Impact of Aspect Ratios on Pressure Drop in Rectangular Micro\_channel(in Chinese)[J]. Chinese Hydraulics & Pneumatics, 2009, (01): 17-19.
- [14]. Bhattacharyya S, Chattopadhyay H, Swami A, et al. Convective Heat Transfer Enhancement and Entropy Generation of Laminar Flow of Water through a Wavy Channel[J]. International Journal of Heat and Technology, 2016, 34(4): 727-733.
- [15]. Aroonrat K, Wongwises S. Experimental investigation of condensation heat transfer and pressure drop of R-134a flowing inside dimpled tubes with different dimpled depths[J]. International Journal of Heat and Mass Transfer, 2019, 128: 783-793.